JVI Journals.ASM.org

Human Galectin 3 Binding Protein Interacts with Recombinant Adeno-Associated Virus Type 6

Jerome Denard,[a] Cyriaque Beley,[b] Robert Kotin,[c] René Lai-Kuen,[d] Stéphane Blot,[b,e] Hervé Leh,[f] Aravind Asokan,[g] R. Jude Samulski,[g] Philippe Moullier,[a,h,i] Thomas Voit,[b] Luis Garcia,[b] and Fedor Svinartchouk[a]

Genethon, Evry, France[a]; Université Pierre et Marie Curie, Um76, Inserm U974, CNRS UMR7215, Institut de Myologie, Paris, France[b]; Molecular Virology and Gene Therapy Laboratory, Genetics and Developmental Biology Center, National Heart, Lung, and Blood Institute, National Institutes of Health, Bethesda, Maryland, USA[c]; Technical Platform of the IFR71/IMTCE-Cellular and Molecular Imaging, Faculty of Pharmacy, Paris Descartes University, Paris, France[d]; Université Paris-Est Créteil, École Nationale Vétérinaire d'Alfort, UPR de Neurobiologie, Maisons-Alfort, France[e]; LBPA, École normale supérieure de Cachan, CNRS, Cachan, France[f]; Gene Therapy Center, University of North Carolina School of Medicine, Chapel Hill, North Carolina, USA[g]; Université de Nantes, Inserm UMR649, Nantes, France[h]; and Molecular Genetics and Microbiology Department, University of Florida, Gainesville, Florida, USA[i]

Recombinant adeno-associated viruses (rAAVs) hold enormous potential for human gene therapy. Despite the well-established safety and efficacy of rAAVs for *in vivo* gene transfer, there is still little information concerning the fate of vectors in blood following systemic delivery. We screened for serum proteins interacting with different AAV serotypes in humans, macaques, dogs, and mice. We report that serotypes rAAV-1, -5, and -6 but not serotypes rAAV-2, -7, -8, -9, and -10 interact in human sera with galectin 3 binding protein (hu-G3BP), a soluble scavenger receptor. Among the three serotypes, rAAV-6 has the most important capacities for binding to G3BP. rAAV-6 also bound G3BP in dog sera but not in macaque and mouse sera. In mice, rAAV-6 interacted with another protein of the innate immune system, C-reactive protein (CRP). Furthermore, interaction of hu-G3BP with rAAV-6 led to the formation of aggregates and hampered transduction when the two were codelivered into the mouse. Based on these data, we propose that species-specific interactions of AAVs with blood proteins may differentially impact vector distribution and efficacy in different animal models.

The recombinant adeno-associated vector (rAAV) platform, derived from a nonpathogenic dependovirus, has many attributes suitable for *in vivo* gene transfer: rAAV vectors are capable of transducing a wide range of cell types, including dividing and nondividing cells; rAAV genomes persist as episomal chromatin in the nucleus of transduced cells (38); and stable, persistent expression has been reported for many transgenes in different tissues and species (6, 12, 36, 39). rAAVs have proven to be efficient in preclinical studies in animal models (16, 28), and results from clinical trials are promising (7, 47).

In the case of systemic diseases, clinical relevance requires widespread distribution of the vector in order to target entire organs. This is particularly true for myopathies, where all striated muscles of the skeletal musculature and, frequently, cardiac muscles have to be treated. In this case, vascular delivery would be the optimal route for rAAV administration. Intravascular injection of a number of rAAV serotypes has proven efficient in murine models of muscular dystrophies (11, 17, 18, 34, 35). However, translating this approach to large animal models and humans is still challenging. Acquired immunity and neutralizing antibodies present in a large fraction of the human population might obviously be restrictive for rAAV gene delivery (5, 20, 27, 29, 30). Moreover, recent studies have demonstrated that serum might also contain other factors neutralizing rAAV vectors (40), indicating that detailed characterization of rAAV's molecular interactions in the bloodstream is obviously important in order to improve vector efficacy.

We looked for serum proteins, other than immunoglobulins, which could interact with rAAVs in the bloodstreams of different species. By using a multidisciplinary approach involving proteomics, binding assays, electron microscopy (EM), and *in vivo* studies, we demonstrated that rAAV-6 interacted specifically with C-reactive protein (CRP) in mice and galectin 3 binding protein (G3BP) in humans and dogs. Interestingly, CRP belongs to the short pentraxins, whose main functions are to recognize a variety of pathogenic agents (2), and G3BP contains a scavenger receptor cysteine-rich (SRCR) domain, which plays an important role in uptake and clearance of weakened components, such as modified host molecules and apoptotic cells (26, 37). We found that in human serum human G3BP (hu-G3BP) was able to aggregate and precipitate rAAV-6. More importantly, this protein was able to reduce rAAV-6 transduction efficiency when administered intramuscularly or intravenously in the mouse. Taken together, these results demonstrate that rAAV vectors can interact with serum proteins in a species-specific manner and that this phenomenon should be taken into consideration regarding vector distribution/efficacy in different animal models.

MATERIALS AND METHODS

rAAV production. Pseudotyped rAAV vectors were generated by packaging AAV2-based recombinant genomes into rAAV-1, -2, -5, -6, -8, -9, and -10 capsids using previously described methods. Adenovirus-free vectors were generated either by using a three-plasmid transfection of HEK293 cells (rAAV-1, -2, -5, -6, -9, and -10) (13, 50) or by double infection of Sf9 cells (rAAV-6, -8, and -9) (44). rAAV vectors were purified either by affinity chromatography using AVB Sepharose HP (IA beads) (GE

Received 6 February 2012 Accepted 2 April 2012
Published ahead of print 11 April 2012
Address correspondence to Luis Garcia, luis.garcia@upmc.fr, or Fedor Svinartchouk, svinart@genethon.fr.

doi:10.1128/JVI.00297-12

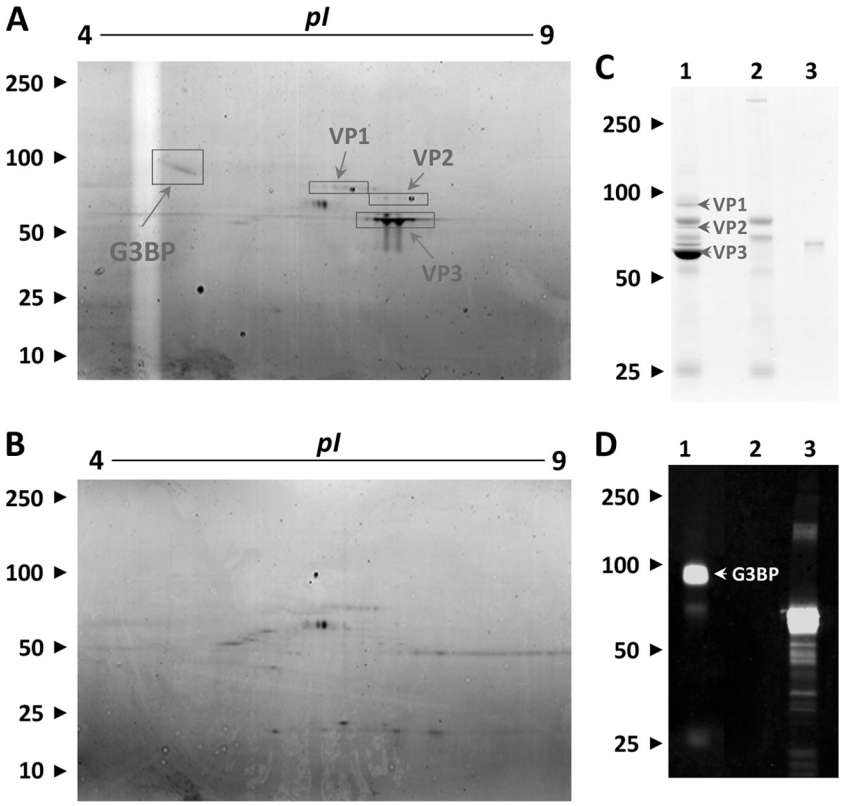

FIG 1 Proteomic analysis of human serum proteins interacting with rAAV-6. (A and B) Human serum proteins recovered by coimmunoprecipitation with AVB-Sepharose immunoaffinity beads in the presence (A) or absence (B) of rAAV-6 (10E12 physical particles) and analyzed by 2-DE. In the presence of rAAV-6, in addition to the AAV capsid proteins, VP1, VP2, and VP3, a number of protein spots with similar molecular masses (about 90 kDa) and isoelectric points (5.1 to 5.2) were reproducibly detected (5 experiments), but they were not seen in the absence of rAAV-6. MALDI-TOF analysis identified these spots as human galectin 3 binding protein (hu-G3BP). Identification of G3BP was confirmed by Western blot analysis. (C) Coomassie blue staining of SDS-PAGE gel. (D) Corresponding polyvinylidene difluoride (PVDF) membrane probed with a goat polyclonal antibody against hu-G3BP (1:1,000; R&D Systems). Lanes 1 and 2, protein extracts from human serum recovered via AVB immunoaffinity beads with rAAV-6 or beads alone, respectively. Lane 3, 100 ng of recombinant nonglycosylated G3BP (65-kDa molecular mass). The AAV capsid proteins, VP1, VP2, and VP3, as well as serum hu-G3BP (around 90 kDa in molecular mass), were found in lane 1. Two faint bands of about 70 kDa and 26 kDa, corresponding to N-terminal and C-terminal fragments, were generated by proteolytic cleavage of hu-G3BP (26, 42). In lane 2, empty beads did not retain hu-G3BP, although some proteins could be recovered depending on washing stringency. Numbers to the left of each panel are molecular masses in kilodaltons.

Healthcare Life Sciences, Piscataway, NJ) (44) or by a standard procedure including two cycles of cesium chloride or iodixanol gradient centrifugation (22). The number of viral genomes (vg) was estimated by quantitative PCR (qPCR) of extracted vector DNA. The numbers of vector physical particles (pp) were estimated either by an enzyme-linked immunosorbent assay (ELISA)-based method or by quantification of VP3 protein after SDS-PAGE analysis of samples stained with Coomassie blue G250 with bovine serum albumin (BSA) as a standard. Contents of full capsids were very similar for the different serotypes used in the study: the ratio of viral genomes to physical particles varied from 1/3 to 1/10.

Animals. Healthy, 4-week-old C57BL/6 mice were used in the study. All the procedures involving animals were performed according to the guidelines of the Animal Ethical Committee of our institute. All experiments were performed at least in duplicate and some in triplicate, with at least three mice used for each condition. For systemic delivery, 6 × 10E11 vg of rAAV-6 or 1 × 10E11 vg of rAAV-9 (prepared by triple transfection of 293 cells and purified by ultracentrifugation on iodixanol) coding for the murine secreted embryonic alkaline phosphatase (MuSEAP) (49) under the cytomegalovirus (CMV) promoter were injected into the lateral tail vein. For intramuscular delivery, the following quantities of vectors were injected into the left tibialis anterior (TA) muscle after anesthesia by intraperitoneal injection of ketamine (100 mg/kg of body weight; Virbac) and xylazine (10 mg/kg; Rompun): 5 × 10E9 vg of rAAV-6, rAAV-7, and rAAV-1 or 1 × 10E9 vg of rAAV-9 coding for MuSEAP. Vectors and hu-G3BP at the physiological concentration were incubated for 1 h at ambient temperature before injections. The final volume was adjusted to 120 μl or 20 μl with phosphate-buffered saline (PBS) for intravenous and intramuscular injections, respectively. Mice were sacrificed 2 weeks after injection, and serum levels of MuSEAP were evaluated by chemiluminescence reporter assay (Tropix, Bedford MA).

Sera. Commercially available human serum (Sigma, St. Louis, MO) or serum samples from healthy human adults obtained in accordance with regulatory guidelines were used in the experiments. Canine sera were obtained from two healthy golden retriever dogs of 6 and 9 months of age (Ecole Nationale Vétérinaire d'Alfort). Macaque (*Macaca fascicularis*) sera were obtained from the Ecole Nationale Vétérinaire de Nantes. Sera used in this study were assessed for the presence of antibodies according to the method in reference 5 and were seronegative for the respective AAV serotypes. Before coprecipitation assays, sera were processed by ultracentrifugation at 230,000 × *g* for 2 h (Beckman 100 ultracentrifuge; TLA 100.4 rotor).

Coprecipitation experiments. Serum proteins interacting with rAAV were coprecipitated from processed serum by ultracentrifugation at 40,000 × *g* for 2 h at room temperature (Beckman 100 ultracentrifuge; TLA 100.4 rotor). Pellets were washed with 4.7 ml of PBS and reprecipitated under the same conditions. The resulting precipitates were resus-

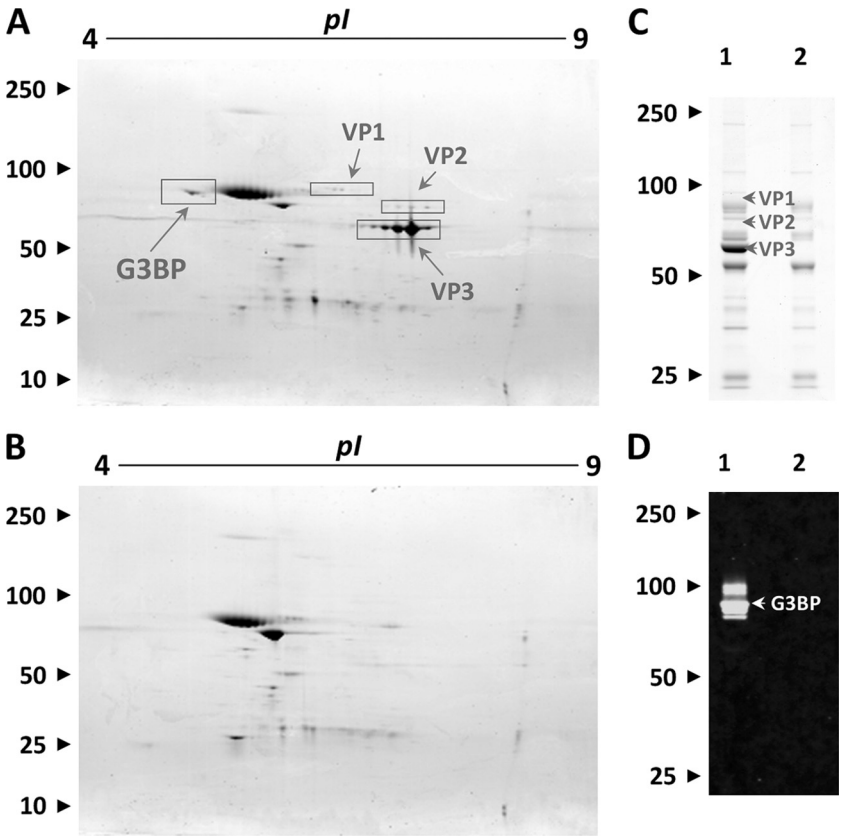

FIG 2 Proteomic analysis of dog serum proteins interacting with rAAV-6. (A and B) Dog serum proteins recovered by ultracentrifugation in the presence (A) or absence (B) of rAAV-6 (10E12 physical particles) and analyzed by 2-DE. In the presence of rAAV-6, in addition to the AAV capsid proteins, VP1, VP2, and VP3, a number of protein spots with similar molecular masses (about 85 kDa) and isoelectric points (5.0 to 5.2) were reproducibly detected (4 experiments), but they were not seen in the absence of rAAV-6. MALDI-TOF analysis identified these spots as dog galectin 3 binding protein (G3BP). Identification of G3BP was confirmed by coimmunoprecipitation with AVB-Sepharose immunoaffinity beads followed by Western blot analysis. (C) Coomassie blue staining of SDS-PAGE gel. (D) Corresponding polyvinylidene difluoride (PVDF) membrane probed with a rabbit polyclonal antibody against the rat protein homolog of G3BP, CyCAP (1:500; Immuno-Biological Laboratories Co., Ltd., Minneapolis, MN). Lanes 1 and 2, protein extracts from human serum recovered via AVB immunoaffinity beads with rAAV-6 or beads alone, respectively. The AAV capsid proteins, VP1, VP2, and VP3, as well as serum dog G3BP (around 80 kDa in molecular mass), were found in lane 1. In lane 2, empty beads did not retain hu-G3BP, although some proteins could be recovered depending on washing stringency. Multiple bands revealed by the antibody could be due to the variable pattern of dog G3BP glycosylation. Numbers to the left of each panel are molecular masses in kilodaltons.

pended in 200 μl of PBS, and proteins were precipitated with 2 volumes of cold acetone. For two-dimensional gel electrophoresis (2-DE), proteins were dissolved in 180 μl of rehydration buffer (7 M urea, 2 M thiourea, 1% [vol/vol] Triton X-100, 1% [wt/vol] amidosulfobetaine-14 [ASB-14], 2% [wt/vol] 3-[(3-cholamidopropyl)-dimethylammonio]-1-propanesulfonate [CHAPS], and 20 mM dithiothreitol [DTT]).

Coimmunoprecipitation. Coimmunoprecipitation of serum proteins was performed with rAAV vectors immobilized on AAV capsid-specific immunoaffinity beads (AVB-Sepharose beads; GE Healthcare Life Sciences, Piscataway, NJ)) (4). Immobilized rAAV vectors (5 μl of AVB Sepharose/1 × 10E12 vector particles) were incubated with 400 μl of serum for 1 h. Beads were collected by centrifugation and washed four times with 1× PBS. The immunoprecipitate was solubilized in the appropriate buffer for further analysis by one-dimensional (1-D) or 2-D electrophoresis.

Low-speed centrifugation. Putative aggregate formation with rAAV-6, -1, and -9 was assessed by low-speed centrifugation. The respective rAAV (2 × 10E11 physical particles alone or with hu-G3BP at 20 μg/ml) was incubated in 80 μl of PBS containing 20 μg/ml of hu-G3BP for 1 h and centrifuged at 2,000 × *g* for 10 min, and then the supernatant (70 μl) was carefully discarded. Ten-microliter aliquots from the supernatant and precipitate were analyzed by SDS-PAGE. Repartition of rAAV in the two compartments was estimated by Coomassie blue staining of viral proteins.

Serum depletion of G3BP. Human serum was depleted of G3BP by incubation with anti-G3BP antibodies bound to magnetic beads for 2 h at room temperature. Coupling of anti-G3BP SP-2 mouse monoclonal IgG1 (MediaPharma, Italy) to activated magnetic beads (Dynabeads M-450 Tosylactivated; Invitrogen, Oslo, Norway) was performed according to the manufacturer's instructions. Five micrograms of antibody was used in a reaction mixture with 25 μl of magnetic beads.

G3BP purification from human serum. Human G3BP was purified with anti-G3BP antibodies bound to the magnetic beads. The beads were washed extensively with PBS supplemented with 0.5% Triton X-100, followed by PBS. The adsorbed proteins were eluted in 200 mM Tris buffer, pH 9.5. Typically, 2.5 μg of hu-G3BP per 1 ml of serum was obtained.

2-DE and protein identification. Two-dimensional gel electrophoresis (2-DE) analysis, Coomassie blue staining, and identification of proteins separated by 2-DE were performed as previously described (10). Tryptic monoisotopic peptide masses were searched by using Aldente software (version 11 February 2008) in the UniProtKB/Swiss-Prot database (release 56.9 of 3 March 2009) or by Protein Prospector (http://prospector.ucsf.edu) in the NCBI (25 November 2008) and UniProtKB (10 June 2008) databases with the

following parameters: human/mouse/dog species, one missed cleavage site, and mass tolerance setting of 20 ppm. Partial chemical modification such as oxidation of methionine was taken into consideration for the queries. Highest-confidence identifications have statistically significant search scores, are consistent with the gel region from which the protein was excised (molecular weight [MW] and pI), and account for the extent of sequence coverage and the number of peptides matched.

Western blot analysis. Protein samples were separated by electrophoresis onto a 4 to 12% gradient SDS-polyacrylamide gel and transferred onto a PVDF-Plus polyvinylidene difluoride (PVDF) membrane (Millipore). The following primary antibodies were used: goat polyclonal antibody to hu-G3BP (1:1,000; R&D Systems); goat polyclonal antibody to mouse CRP (1:1,000; R&D Systems), mouse monoclonal antibody to human CRP (1:250; R&D Systems), and rabbit polyclonal antibody to the rat protein homolog of G3BP, CyCAP (1:500; Immuno-Biological Laboratories Co., Ltd., Minneapolis, MN) followed by corresponding IRDye-800CW- or IRDye-600CW-conjugated antibodies (1:10,000) according to the manufacturer's instructions (Li-Cor Bioscience). Infrared fluorescence of the secondary antibodies was read on an Odyssey imaging system.

Estimation of rAAV-6/hu-G3BP ratios in the complexes. The rAAV-6/hu-G3BP ratio was estimated by quantifying the amount of rAAV-6 and hu-G3BP in coprecipitates. Amounts of rAAV were evaluated by estimating VP3 protein content on corresponding SDS-PAGE gels after Coomassie blue staining, using the known quantity of rAAV-6 as a standard, while G3BP was estimated by Western blot analysis using known quantities of hu-G3BP (GenWayBio) as a standard.

Transmission electron microscopy. Aliquots of vectors (10E11 physical particles) were incubated in the presence of either (i) 10 μg/ml of BSA, (ii) BSA plus 1 μg/ml of hu-G3BP, or (iii) BSA plus 10 μg/ml of hu-G3BP for 1 h. Vector particles (1 × 10E11 physical particles) or the mixtures with hu-G3BP were applied to Formvar-coated copper grids and then negatively stained with 3% uranyl acetate. Images were obtained with a JEOL JEM-100S transmission electron microscope (magnification from ×50,000 to ×100,000).

SPRi. Experiments were performed using a surface plasmon resonance imagery (SPRi) machine from Genoptics. Vectors (0.2 μl of 10^{12} to 10^{13} pp/ml) were immobilized on a glass prism as described before (33). A dose-dependent binding study was performed using several dilutions of hu-G3BP (10 nM, 20 nM, and 40 nM) with PBS as a running buffer, and then the rAAV surface was regenerated by injection of 100 μl of 25 mM NaOH (8). In order to determine the kinetic constants, SPRi data were analyzed with BiaEvaluation software (Biacore) by using a 1:1 Langmuir binding model. Data from four different concentrations of hu-G3BP were used for the analysis, and the experiment was repeated three times.

RESULTS

rAAV-6 interacts with G3BP in human and dog sera but not in macaque serum. Association of serum proteins with purified rAAV-6 was tested in human serum samples from AAV-6 antibody-seronegative individuals. Proteins interacting with vectors were recovered via rAAV-6 immobilized on immunoaffinity AVB-Sepharose beads followed by 2-D gel analysis. In a reproducible manner, 2-D gels revealed numerous specific spots with similar molecular masses (about 90 kDa) and isoelectric points (5.1 to 5.2) when incubated in the presence of AAV vector (Fig. 1A and B). These spots were identified as human galectin 3 binding protein (hu-G3BP) by matrix-assisted laser desorption ionization–time of flight (MALDI-TOF) analysis (12/35 peptide matching [33%]; 21% of coverage; MOWSE score, 1.58 × 10E6). In addition to G3BP, a number of other spots were observed on the 2-D gels, and the most abundant of these spots were identified by mass spectrometry as albumin, heavy and light chains of IgG, and μ chain of IgM. Since all of them were also found in control experiments without AAV particles (proteins that bind empty AVB beads), these spots were not considered relevant for interaction with AAV vectors. Identification of rAAV-6-associated hu-G3BP was further confirmed by Western blot analysis (Fig. 1C and D).

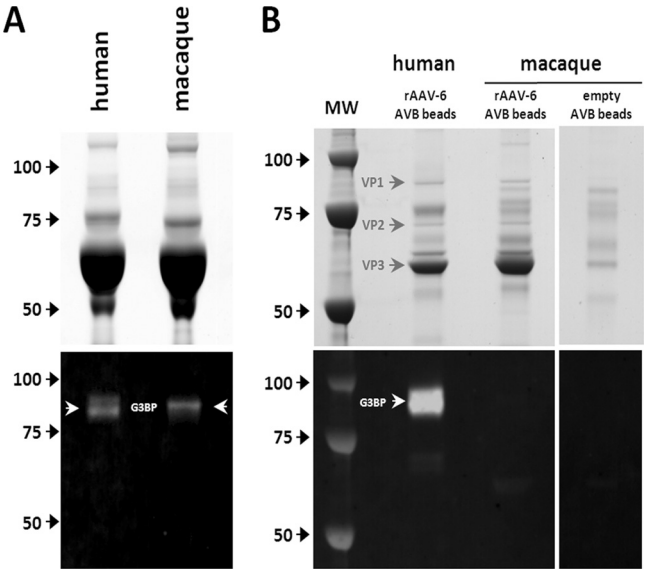

FIG 3 Macaque G3BP does not interact with rAAV-6. Western blot analysis of 0.3 μl of total serum from human and macaque demonstrated that macaque G3BP is recognized by the anti-hu-G3BP antibody (A). Western blot analysis with anti-G3BP antibody of proteins from macaque serum recovered via rAAV-6 immobilized on AVB-Sepharose beads. Human serum on rAAV-6 beads was used as a positive control (B). (Top) Coomassie blue staining; (bottom) corresponding Western blot analysis. Numbers to the left of each panel are molecular weights (MW).

Golden retriever muscular dystrophy (GRMD), the canine model of Duchenne muscular dystrophy (DMD), is often used to assess AAV-based therapy for DMD (4, 25). We tested whether the G3BP of golden retrievers was also capable of interacting with rAAV-6 similarly to its human homolog. Association of serum proteins with purified rAAV-6 was tested in serum samples from AAV-6 antibody-seronegative dogs by using either cosedimentation or coimmunoprecipitation methods followed by 2-D gel analysis. Similar to what was observed in human sera, 2-D gels exhibited multiple specific spots with an apparent molecular mass of 85 kDa and a pI of 5.1 (Fig. 2A and B). These spots were also identified as G3BP by MALDI-TOF analysis. The higher mobility of dog G3BP than of hu-G3BP can be explained by the smaller size of this protein (559 amino acids versus 585 in human) and also by differences in glycosylation. Identification of rAAV-6-associated dog G3BP was further confirmed by Western blot analysis (Fig. 2C and D).

In view of the fact that the macaque is often considered a relevant model in preclinical gene therapy studies, we tested whether the G3BP of *Macaca fascicularis* origin (98% of identity with hu-G3BP) interacts with rAAV-6 similarly to its human and dog homologs. Although the macaque G3BP was recognized by a polyclonal anti-hu-G3BP antibody, Western blot analysis of serum samples investigated after immunoprecipitation with rAAV-6 showed, surprisingly, no detectable interaction with macaque G3BP (Fig. 3A and B).

rAAV-6 does not interact with G3BP but with CRP in mouse serum. Following similar experiments with mouse (C57BL/6) se-

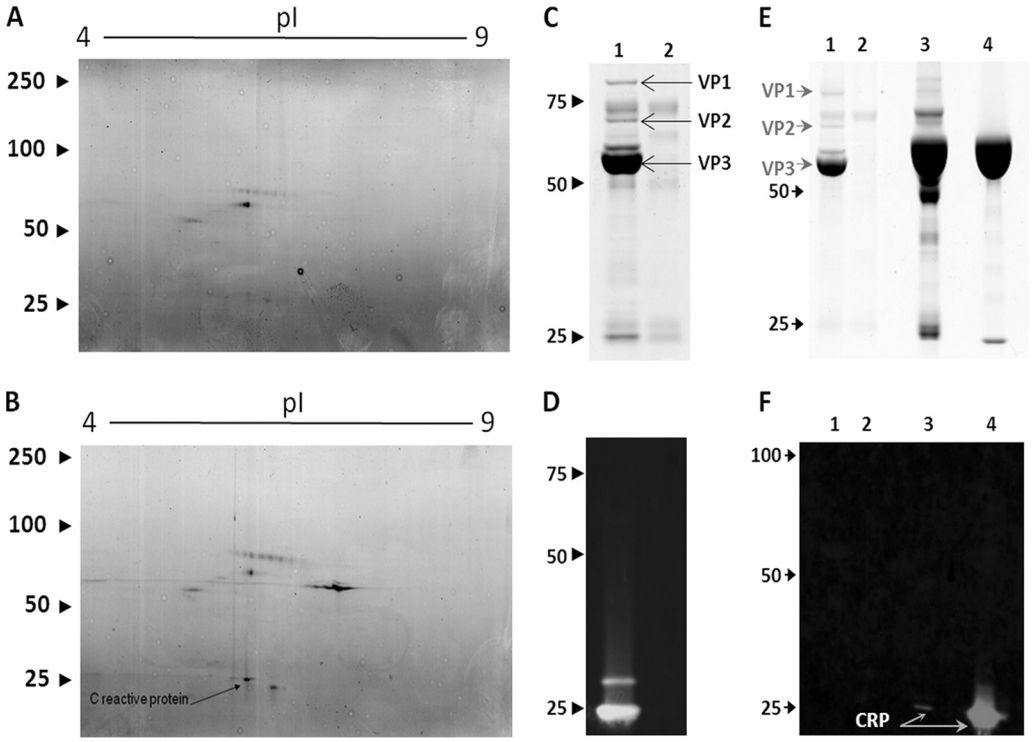

FIG 4 CRP, but not G3BP, interacts with rAAV-6 in mouse serum. 2-DE of mouse serum proteins recovered with AVB-Sepharose immunoaffinity beads alone (A) or with rAAV-6 (B). An additional protein of about 25 kDa was eluted from AVB-Sepharose in the presence of rAAV-6 and identified by MALDI-TOF analysis as C-reactive protein (CRP). Identification of CRP was confirmed by Western blot analysis: Coomassie blue staining of SDS-PAGE gel (C) and corresponding Western blot analysis using a goat anti-mouse polyclonal antibody (D). Lanes 1 and 2, protein extracts from mouse serum recovered via rAAV-6/AVB-Sepharose or AVB-Sepharose alone, respectively. VP1, VP2, and VP3, as well as serum CRP (around 25 kDa in molecular mass), were detected in lane 1. In lane 2, beads alone did not retain CRP, although some other unidentified proteins were recovered depending on washing stringency. The human homolog of mouse CRP does not interact with rAAV-6 (Coomassie blue staining of SDS-PAGE gel [E] and corresponding Western blot analysis [F]). While anti-human CRP antibodies were efficient at visualizing CRP in human serum, no such protein was recovered in the presence of rAAV-6 preadsorbed to AVB-Sepharose. Lane 1, proteins recovered in the presence of rAAV-6 preadsorbed to AVB-Sepharose; lane 2, serum proteins retained by AVB-Sepharose beads alone; lane 3, unfractionated human serum; lane 4, recombinant CRP (100 ng) stabilized with BSA. Numbers to the left of each panel are molecular masses in kilodaltons.

rum, we did not detect spots corresponding to the murine protein homolog of G3BP (i.e., the mouse cyclophilin C-associated protein, 68% homology to hu-G3BP, with an apparent molecular mass of 77 kDa on SDS-PAGE and pI 5.0 [9, 14]) (Fig. 4A and B). Instead of G3BP, protein immunoprecipitation experiments with rAAV-6 readily detected a spot with a molecular mass of 24 kDa (Fig. 4A and B). This spot was subsequently identified by MALDI-TOF analysis as the mouse C-reactive protein (CRP). Retention of the murine CRP by rAAV-6 was further confirmed by Western blot analysis (Fig. 4C and D). Importantly, human CRP did not react with rAAV-6 (Fig. 4E and F), thus demonstrating that this AAV serotype interacted with serum proteins in a species-specific manner.

Human G3BP interacts differentially with rAAV serotypes. We further investigated interactions of several serotypes (rAAV-1, -2, -5, -6, -7, -8, -9, and -10 and an rAAV-2/rAAV-8 chimera named rAAV-2i8 [3]) with G3BP in the respective human antibody-seronegative sera. Immobilized on AVB-Sepharose beads, rAAVs were incubated with relevant sera, and the resulting hu-G3BP binding was determined by Western blot analysis. For rAAV-9, which does not bind AVB-Sepharose beads, putative complexes were assessed by cosedimentation. Noticeably, hu-G3BP was recovered in the presence of rAAV-1, -5, and -6 but not in the presence of rAAV-2, -2i8, -7, -8, -9, and -10 (Fig. 5A and B). Binding affinities of rAAV-6 and -9 for hu-G3BP were further analyzed by using surface plasmon resonance imagery (SPRi) (Fig. 5D). Again, rAAV-9 did not show any binding, while rAAV-6 displayed an association constant (K_A) for hu-G3BP of $\approx$10E9 M^{-1}.

Binding capacities of rAAV-1, -5, and -6 for hu-G3BP were different. Three to five times less G3BP was bound by rAAV-1 or rAAV-5 than by rAAV-6 (Fig. 5A). Interestingly, only six amino acid residues differ between AAV-1 and AAV-6 VP1 proteins, suggesting that an important molecular determinant for hu-G3BP binding could lie within these amino acid residues. The K531 residue is unique to AAV-6 among currently known serotypes, which contain a conserved glutamate or aspartate residue at the corresponding 531 position. We tested the significance of this residue in hu-G3BP recovery by swapping amino acids at position 531 between rAAV-1 and rAAV-6. As shown in Fig. 5C, such modifications affected hu-G3BP binding: the rAAV-1(E531K) mutant increased its hu-G3BP binding capacity nearly to the level of rAAV-6, while rAAV-6(K531E) decreased to the level of rAAV-1. These results confirmed that lysine 531 was a key determinant for hu-G3BP binding. However, since this residue was previously identified as a heparin-binding determinant on rAAV-6 capsids

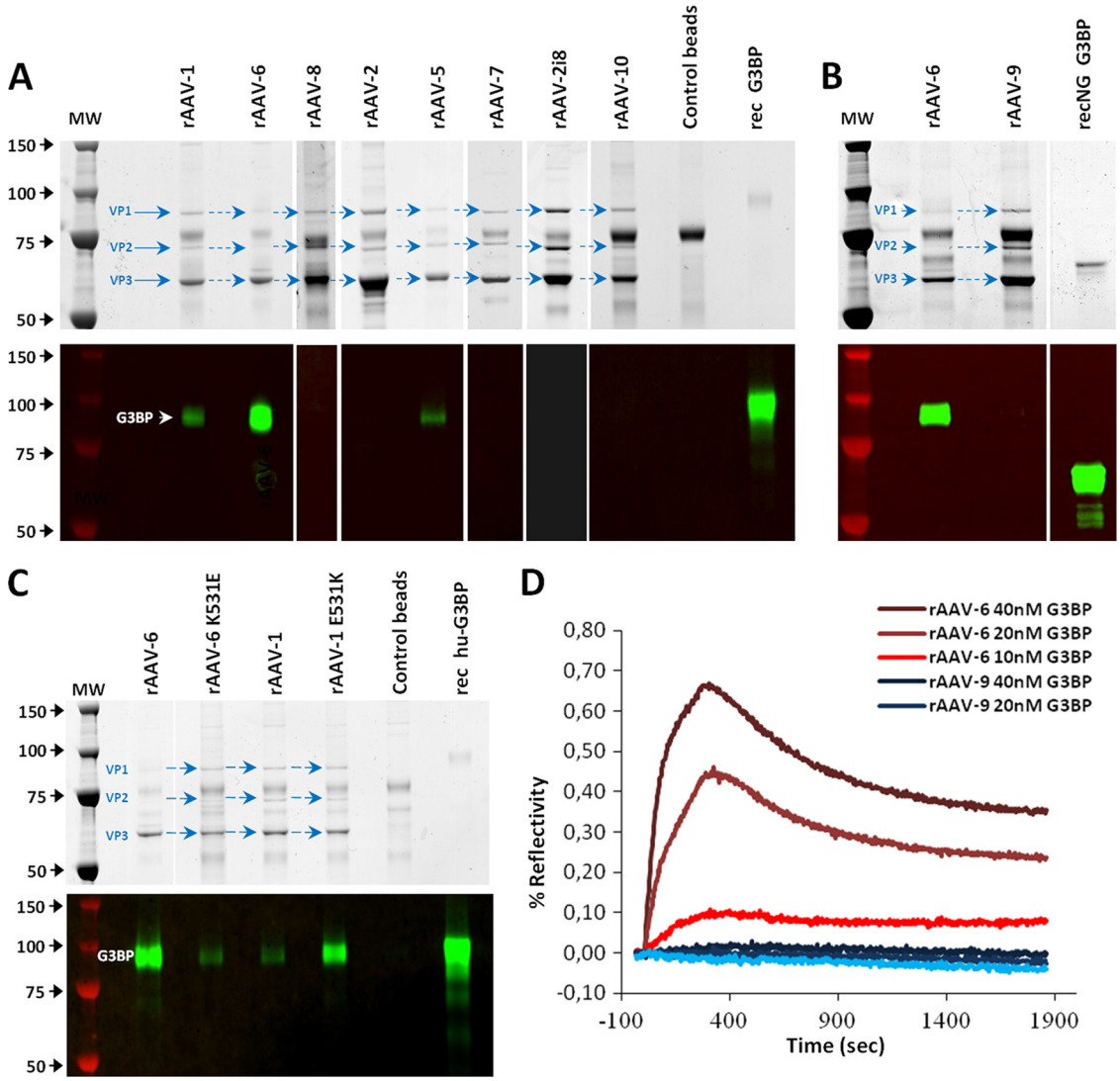

FIG 5 Interaction of hu-G3BP with different serotypes of rAAV. (A) Interactions of human G3BP with different rAAV serotypes were assessed by SDS-PAGE and Western blot analysis of serum proteins retained on rAAVs immobilized on AVB-Sepharose beads. (B) In the case of rAAV-9, interaction with hu-G3BP was assessed by coprecipitation from serum by ultracentrifugation. (C) Interaction of rAAV mutants with hu-G3BP after swapping amino acids at position 531 between rAAV-1 and rAAV-6. MW, molecular weight standard. rAAV serotypes are designated above the lanes. Control beads, AVB-Sepharose beads without rAAV; rec hu-G3BP, recombinant glycosylated human protein; recNG G3BP, recombinant nonglycosylated human protein. Positions of hu-G3BP and viral capsid proteins are indicated by arrows. (D) Interactions of hu-G3BP with rAAV-6 and -9 were assessed by surface plasmon resonance imagery. rAAV vectors were immobilized on glass prisms, and a dose-dependent binding study was performed using 10, 20, and 40 nM hu-G3BP.

(51), we wondered whether binding to heparin and that to hu-G3BP affected each other. Competition experiments with up to 100 μg/ml of heparin (molar excess of 100 over G3BP) showed no effect of heparin on hu-G3BP recovery by rAAV-6 (Fig. 6).

Human G3BP aggregates rAAV-6. Aggregation of rAAV-6 in the presence of purified hu-G3BP was assessed by electron microscopy (EM). rAAV-6 was diluted until vector particles appeared as individual units scattered over the grid (Fig. 7A). In the presence of 1 μg/ml hu-G3BP, small aggregates containing 15 to 200 vector particles were observed (Fig. 7B). At 10 μg/ml hu-G3BP, which corresponds to the G3BP physiological concentration in human blood (ranging from 1.3 to 17 μg/ml), large electron-dense structures were formed (Fig. 6C). These structures were made of numerous vector particles aggregated with hu-G3BP as evidenced by anti-G3BP immunogold staining (data not shown). Consistent with our binding assay data, rAAV-9 never formed such structures in the presence of hu-G3BP (Fig. 7D, E, and F).

The propensity of vectors to aggregate with hu-G3BP was also assessed by comparing vector recoveries in supernatant and pellet fractions after low-speed centrifugation (Fig. 7G). According to this experimental procedure, the respective rAAV was incubated in 80 μl of PBS or PBS containing 20 μg/ml of hu-G3BP for 1 h, and after centrifugation at 2,000 × *g* for 10 min, the supernatant (70 μl) was carefully discarded. Ten-microliter aliquots from the supernatant and precipitate were analyzed by SDS-PAGE. Vectors were recovered equally in the two fractions in control samples without hu-G3BP. In the presence of 20 μg/ml hu-G3BP, rAAV-6 was preferentially found in the pellet fraction, while rAAV-9 was

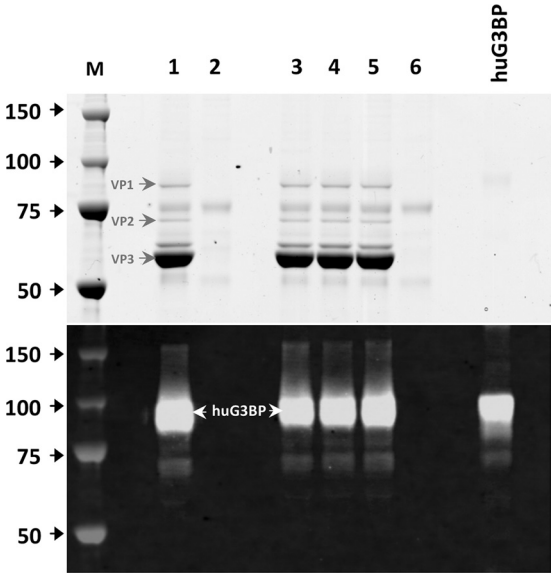

FIG 6 Heparin does not impact hu-G3BP binding to rAAV-6. rAAV-6 immobilized on AVB beads was incubated with human serum in the presence of increasing concentrations of heparin. Interactions of hu-G3BP with rAAV-6 were assessed by SDS-PAGE and Western blot analysis. (Top) Coomassie blue staining of VP proteins of rAAV-6. (Bottom) Western blot analysis of hu-G3BP bound to rAAV-6. M, molecular weight standard; lane 1, rAAV-6 immobilized on AVB beads and incubated with human serum; lane 2, AVB-Sepharose beads without rAAV incubated with human serum; lanes 3, 4, and 5, rAAV-6 immobilized on AVB beads and incubated with human serum in the presence of heparin at 1, 10, and 100 μg/ml, respectively; lane 6, AVB beads without rAAV incubated with human serum in the presence of 100 μg/ml of heparin. Hu-G3BP, 100 ng of recombinant glycosylated human G3BP.

detected equally in the pellet fraction and the supernatant. Intriguingly, rAAV-1 was not precipitated despite the fact that previous binding assays clearly showed that it could bind hu-G3BP. Aggregation of rAAV-1(E531K) and rAAV-6(K531E) mutants followed their capacities to bind hu-G3BP *in vitro*: the rAAV-1 mutant with Lys in position 531, which efficiently bound hu-G3BP (Fig. 5), was precipitated by the protein, while rAAV-6 with Glu in position 531, which bound hu-G3BP at a lower level, similarly to rAAV-1 (Fig. 5), did not form aggregates precipitated at low-speed centrifugation (Fig. 7).

In order to evaluate a ratio between rAAV-6 and hu-G3BP in the aggregates, VP3 protein in precipitates was estimated after Coomassie blue staining and hu-G3BP content was estimated by Western blot analysis using known quantities of rAAV-6 and recombinant hu-G3BP as standards, respectively. Such quantification allowed us to determine that each rAAV-6 particle could engage two to six hu-G3BP monomers. Importantly, in human serum *per se* G3BP was cosedimented with rAAV-6 under low-speed centrifugation (Fig. 8).

Human G3BP hampers rAAV-6 recovery by immunoaffinity beads. In order to confirm that the properties of rAAV-6 bound to hu-G3BP are different from those of the free rAAV-6, we studied whether hu-G3BP altered recognition of rAAV-6 by AVB-Sepharose beads. For this goal, vectors were preincubated with either PBS supplemented with BSA, human serum, or human serum depleted of hu-G3BP by preincubation with immobilized anti-G3BP antibodies. As expected, recovery of rAAV-6 under the PBS condition was linearly proportional to the concentration of physical vector particles (Fig. 9). In contrast, vector recovery in the presence of human serum was compromised and reduced by up to $1.3 \times 10E12$ physical particles/ml, although a gradual increase was noted, similarly to the PBS condition, at high vector concentrations. When serum was depleted of hu-G3BP, rAAV-6 recovery was similar to that under the PBS condition. These results suggested that hu-G3BP could either change vector surface properties or disable the vector's access to immunoaffinity beads by promoting vector aggregation.

Human G3BP interaction with rAAV-6 impacts transduction efficacy in the mouse. To study the impact of hu-G3BP on transduction efficiency *in vivo*, hu-G3BP and rAAV-6 antibody-seronegative mice (C57BL/6) received intravenous injections of rAAV-6 encoding the murine secreted embryonic alkaline phosphatase (MuSEAP) as a reporter gene, alone or preincubated with purified hu-G3BP at 20 μg/ml. Preincubated rAAV-6 samples were less efficient than control rAAV-6, as illustrated by the 3-fold-lower level of MuSEAP in serum 2 weeks after injection (296 ± 87 ng/ml for rAAV-6/hu-G3BP versus 870 ± 123 ng/ml for rAAV-6 alone) (Fig. 10A).

To further address the effect of circulating hu-G3BP on rAAV-6 transduction efficiency, hu-G3BP was intravenously injected 1 min prior to rAAV-6. By injecting 20 μg of hu-G3BP, we estimated that immediately after injection the peak of circulating hu-G3BP would be about 13 μg/ml, which is in the range of human physiological concentrations (ranging from 1.3 to 17 μg/ml). The results showed that hu-G3BP-preconditioned mice displayed a significant decrease in MuSEAP levels (405 ± 59 ng/ml) compared to that of mice injected with rAAV-6 only (870 ± 123 ng/ml).

On the opposite setting, when rAAV-6 (MuSEAP) was injected before hu-G3BP (1-min interval), subsequent serum levels of MuSEAP were not significantly different from those of controls (842 ± 271 versus 870 ± 123 ng/ml, respectively), suggesting that rAAV-6 might have already reached target organs ahead of the secondary injection of hu-G3BP and was eventually not accessible for aggregation. Consistently, preincubation of rAAV-9 (MuSEAP) with hu-G3BP had no impact on transduction efficiency as shown by unchanged MuSEAP levels (Fig. 10B).

The efficacy of rAAV transduction in the presence of hu-G3BP was also assessed using the intramuscular route of delivery. As shown in Fig. 10C, preincubation of rAAV-6 with hu-G3BP reduced gene delivery to skeletal muscles more than 10-fold, while the same procedure had no effect on vectors which did not bind G3BP, rAAV-7 and rAAV-9. Intriguingly, transduction activity of rAAV-1, which has a lower capacity for binding to G3BP than does rAAV-6, was not affected by preincubation with hu-G3BP (Fig. 10C).

DISCUSSION

It is expected that clinical relevance for gene therapy in the context of systemic muscle diseases would require widespread distribution of gene vectors in order to target the whole skeletal musculature and the heart; in this case, systemic delivery is likely the optimal route of administration. Indeed, body-wide transduction using particular rAAV serotypes (rAAV-1, -6, -8, and -9) has been successfully achieved in rodents (11, 17, 45), and translating this advance to the treatment of larger species such as dystrophic dogs would definitely strengthen the rationale for this approach.

Transduction of large areas of muscle was achieved in mice by using tail vein injections of rAAV-6 (17, 18, 46). In our hands, this

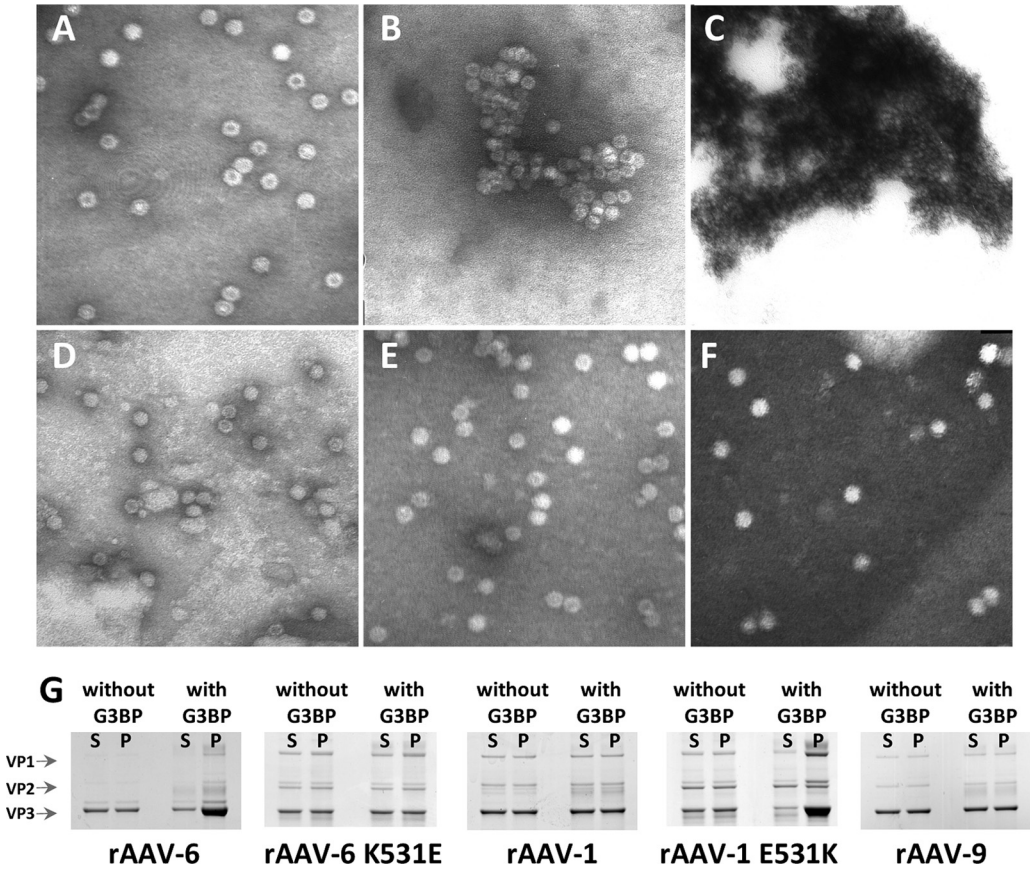

FIG 7 rAAV-6 forms aggregates with hu-G3BP. Formation of hu-G3BP/rAAV complexes was assessed by electron microscopy. (A to C) Aliquots of rAAV-6 (10E11 physical particles) were incubated in the presence of either 10 μg/ml of BSA (A), BSA plus 1 μg/ml of hu-G3BP (B), or BSA plus 10 μg/ml of hu-G3BP (C) for 1 h. Increasing the hu-G3BP concentration enhanced the formation of electron-dense aggregates. (D to F) Electron microscopy analysis of rAAV-9 (10E11 physical particles) in the presence of either 10 μg/ml of BSA (D), BSA plus 1 μg/ml of hu-G3BP (E), or BSA plus 10 μg/ml of hu-G3BP (F). Including hu-G3BP had no effect on the vector aggregation, thus indicating that complexation of hu-G3BP with rAAVs is serotype dependent. (G) Putative aggregate formation with rAAV-6, rAAV-6(K531E), rAAV-1, rAAV-1(E531K), and rAAV-9 was assessed by low-speed centrifugation at 2,000 × *g* for 10 min. Under such conditions, aggregates are preferentially found in pellet (P) while free vectors are recovered in the supernatant (S). Repartition of rAAV in the two compartments was estimated by Coomassie blue staining of viral proteins. Only rAAV-6 and rAAV-1(E531K) were precipitated under such conditions.

vector serotype was also efficient in dogs when we used locoregional limb vector delivery, whereby blood is removed prior to vector infusion or by using percutaneous transendocardial delivery (4), but not after systemic injections. These findings prompted us to investigate whether serum proteins, other than immunoglobulins, could differentially react with rAAV-6 in these species. A recent work has substantiated this hypothesis by showing that depletion of immunoglobulins in dog serum removed their inhibitory effect on rAAV-1 and rAAV-2 transduction but not on rAAV-6 transduction (40). Here, we show that two proteins of the innate immune system, galectin 3 binding protein (G3BP) and C-reactive protein (CRP), interact with different rAAV serotypes in a species-specific manner.

G3BP is a highly glycosylated glycoprotein with all seven potential N-glycosylation sites occupied by complex oligosaccharide chains containing sialic acid (21) but not heparan sulfate (42). The mean concentration of this protein in the plasma of normal children (n = 10) is 6.3 μg/ml (19). Other studies carried out on 100 adults have shown that normal concentrations range from 1.3 to 17 μg/ml (enzyme immunoassay for the quantitative determination of s90K/Mac-2BP in cell culture supernatant; human serum and plasma package insert; IBL International GMBH, Hamburg, Germany; http://www.ibl-international.com/magento/media/catalog/product/B/E/BE59271_IFU_en_s90_MAC-2BP_ELISA_V2011_04_sym2.pdf). From a structural point of view, G3BP is composed of several domains consisting of a single scavenger receptor cysteine-rich (SRCR) domain at the N terminus, two central domains related to the dimerization domains BTP/POZ and IVR of the *Drosophila* kelch protein, and a C-terminal domain (21, 23, 31, 42). The evolutionarily conserved SRCR domain is found in diverse transmembrane and secreted glycoproteins, including CD5, CD6, M130, complement factor 1, and WC1 antigen (41). Many of these proteins are expressed by cells involved in immunity (B cells, T cells, and macrophages) and are implicated in host defense and immune regulation. G3BP interacts with galectin 3 and other extracellular proteins such as collagens IV, V, and VI; fibronectin; and nidogen. The protein forms linear and ring-shaped oligomers. Investigations by scanning transmission electron microscopy have shown that G3BP rings present five to seven 14-nm-long segments made of two 92-kDa G3BP monomers. Although rings vary in size, decamers of about 24 nm in diameter predominate. It is likely that the multivalency of G3BP provided by its assembly into ring-like structures is of decisive importance for the

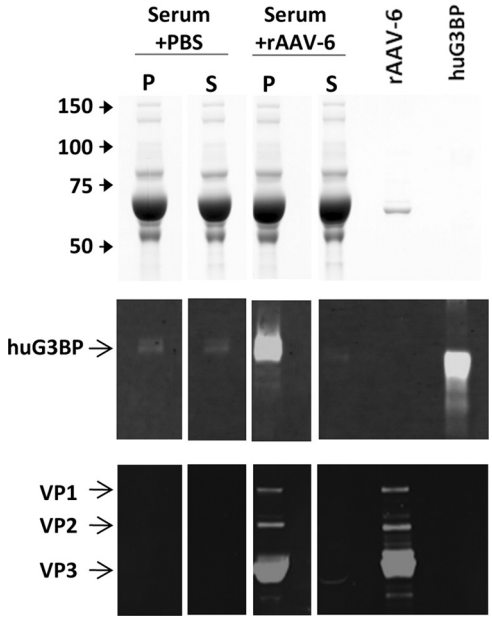

FIG 8 Cosedimentation of rAAV-6 with hu-G3BP in human serum. rAAV-6 ($2 \times 10E12$ pp) was incubated with 400 μl of human serum in a 600-μl total volume for 1 h and then centrifuged at 2,000 × *g* for 10 min. Supernatant (550 μl) was discarded, and precipitate (50 μl) was washed once with 550 μl of PBS and centrifuged at 2,000 × *g* for 10 min. An 0.3-μl amount of the first supernatant and 3 μl (from 50 μl) of the last pellet were analyzed by SDS-PAGE (top) and Western blot analysis (middle) against hu-G3BP or against VP proteins (bottom). In the control experiment, serum was incubated with PBS. P, precipitate; S, supernatant; rAAV-6, 1×10^{11} pp of rAAV-6; rec hu-G3BP, recombinant glycosylated hu-G3BP.

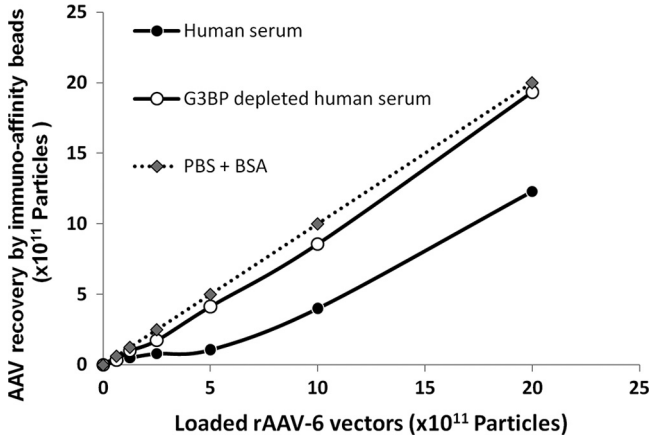

FIG 9 Human G3BP hampers rAAV-6 recovery by AVB beads. Increasing amounts of rAAV-6 (from $1 \times 10E11$ to $2 \times 10E12$ physical particles) were incubated in a 600-μl final volume for 1 h in the presence of either PBS supplemented with 3% BSA, AAV-6-seronegative human serum, or the same serum immunodepleted of G3BP by incubation with anti-G3BP antibodies bound to magnetic beads. The amount of rAAV-6 recovered by AVB-Sepharose was estimated by quantification of the VP3 protein after fractionation by SDS-PAGE and Coomassie blue staining. In the presence of crude serum, vector recovery was partially compromised, thus confirming the presence of an interfering agent. Markedly, rAAV-6 recovery in the G3BP-depleted serum was similar to the PBS condition, which displayed a linear relationship between load and recovery.

linkage of different components and for an increase in binding activity (21, 31).

Estimation of rAAV-6 and hu-G3BP quantities in coprecipitates suggests that each rAAV-6 particle could bind two to six G3BP monomers. This ratio and the possibility of G3BP forming ring-like structures compelled us to propose a 3-D network model where many rAAV-6s are bridged with G3BP rings between them (Fig. 11). Such a network structure could subsequently evolve into large aggregates evidenced by EM and sedimentation analyses. Importantly, 10 μg/ml of hu-G3BP ($\sim 7 \times 10^{13}$ molecules) in human blood is sufficient to react with 0.3×10^{13} rAAV particles/ml as illustrated by rAAV-6 precipitation after incubation with normal human serum (Fig. 8). It is likely that such rAAV-6/G3BP complexes would behave differently from free vectors in crossing the barrier of blood vessels and would affect biodistribution. This hypothesis is in agreement with our *in vivo* results in mice, where the presence of circulating hu-G3BP at physiological levels in the human impacted rAAV-6 transduction, both when administered systemically as a mixture and when administered separately, with hu-G3BP being injected first. Intriguingly, when hu-G3BP was injected only 1 min after rAAV-6, no significant effect was noted on transduction levels, suggesting that either vector dilution in the bloodstream or binding to the vessel walls precluded vector aggregation by hu-G3BP. In contrast to the mouse model, interaction with G3BP could be only one of the first steps of vector recognition in humans, where G3BP is a natural ligand of macrophage-secreted galectin 3, playing an important role in both innate and adaptive immunity. Since ligand binding properties of the human galectin 3 binding protein and its mouse homolog cyclophilin C-associated protein are fairly different (24), the mouse model could reflect only a part of the natural responses in the homologous system.

Interestingly, rAAV-6, which provides whole-body gene transfer in mouse models (18, 46), binds the mouse C-reactive protein (CRP), one of the short pentraxins involved in host defense (1, 15). This protein promotes agglutination, bacterial capsular swelling, phagocytosis, and complement fixation. The lack of efficiency of CRP in blocking rAAV-6 tissue transduction might be due to its low circulating levels in mice (43). Nevertheless, these levels might vary from strain to strain or after stimulation (43) and therefore provide a basis for explaining previously observed variations in transduction efficacy between different mouse models.

The nature of the interaction among different AAV serotypes with hu-G3BP appears to vary significantly. Because vector cleanliness is critical when assaying rAAV properties, we confirmed that these differences were due to the vector serotypes by completing binding assays on multiple brands of vectors made by different laboratories using different methods of production (triple transfection of 293 cells or the baculovirus/Sf9 system) and purified either by density gradient or by AVB immunoaffinity. Importantly, the majority of *in vitro* rAAV/G3BP assays were performed with rAAVs immobilized on AVB beads (except for rAAV-9), which provided additional vector purification. Regardless of the mode of vector production and purification, hu-G3BP–rAAV interactions were highly reproducible, thus confirming that the interactions that we describe here were true vector/host properties and not the result of vector polishing peculiarities.

Interestingly, rAAV-6 formed large aggregates in the presence of hu-G3BP, sedimenting at low speed, while rAAV-1, which dif-

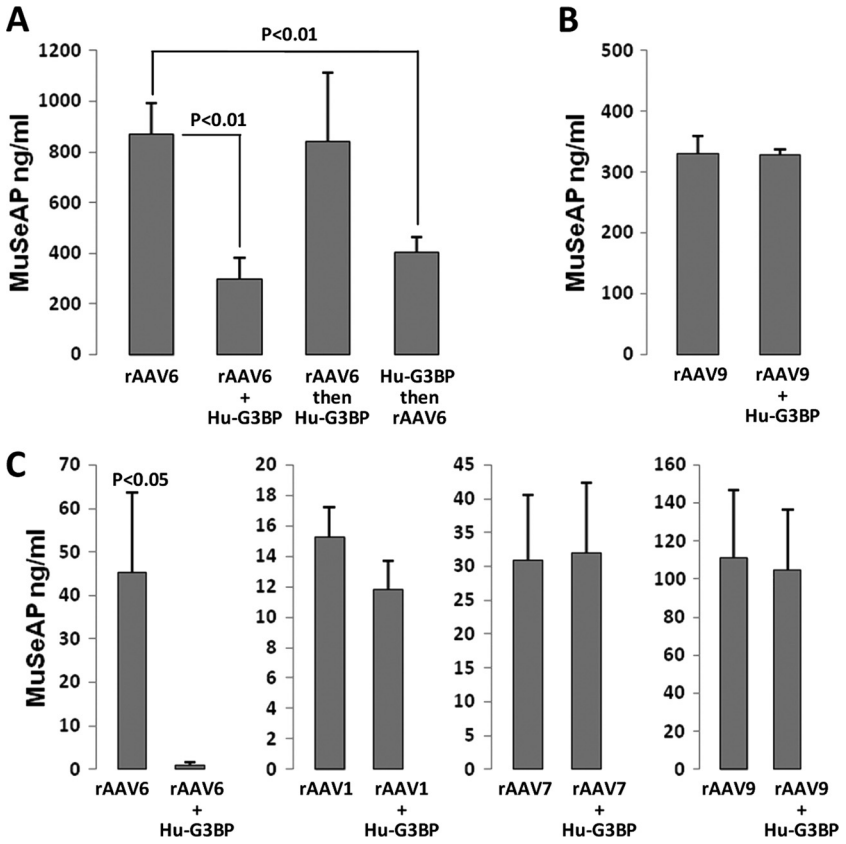

FIG 10 Human G3BP differentially attenuated transduction efficacies of rAAVs following either systemic or intramuscular delivery. (A) Intravenous injections of rAAV-6 MuSEAP. From left to right, 6 × 10E11 vg of rAAV-6 in PBS, 6 × 10E11 vg of rAAV-6 preincubated with hu-G3BP (20 μg/ml), 6 × 10E11 vg of rAAV-6 in PBS followed by an injection of 20 μg of hu-G3BP, and injection of 20 μg of hu-G3BP followed by an injection of 6 × 10E11 vg of rAAV-6. Transduction is expressed as the mean of MuSEAP serum levels (ng/ml) ± standard deviation, 2 weeks after tail vein injection; at least three mice were used for each condition. (B) Intravenous injections of rAAV-9 MuSEAP. (Left) Injection of 10E11 vg of rAAV-9 vectors in PBS; (right) vectors mixed up with 20 μg/ml hu-G3BP. (C) Intramuscular injections of rAAV-6 (5 × 10E9 vg), rAAV-1 (5 × 10E9 vg), rAAV-7 (5 × 10E9 vg), and rAAV-9 (1 × 10E9 vg) coding for MuSEAP. The respective vectors were injected alone or after preincubation with 20 μg/ml hu-G3BP, and transduction was expressed as the mean of MuSEAP serum levels (ng/ml) 2 weeks after injection. Three mice were used for each condition; data are representative of two independent experiments.

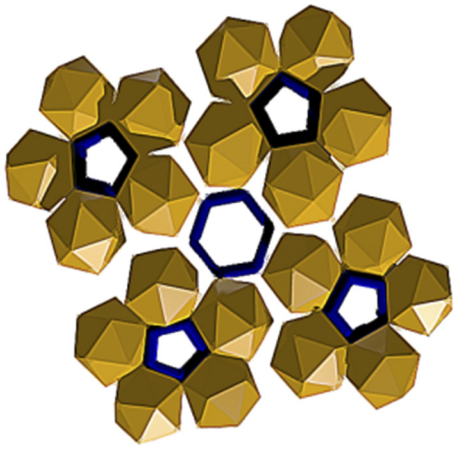

FIG 11 Speculative model of putative interactions between hu-G3BP and rAAV-6. Hu-G3BP makes high-molecular-weight ring structures (blue), potentially bridging several rAAV particles (yellow). Accordingly, hu-G3BP might form a scaffold for a "3D-net" involving a large number of sequestered rAAV particles.

fers from rAAV-6 by only six amino acids, did not show such a phenomenon. Among these residues, the K531 residue, which is known to play a role in heparin binding (32, 51), seems to be crucial for the rAAV-6–G3BP interaction. Nevertheless, dependency on heparin is an unlikely determinant for hu-G3BP: rAAV-2, which also binds heparin sulfate, does not interact with hu-G3BP, and an excess of heparin does not compete with rAAV-6 binding to hu-G3BP.

Taken together, our results demonstrate that rAAV vectors can interact with serum proteins, other than immunoglobulins, in a species-specific manner. We hypothesize that these interactions could play a role in vector efficiency, and recent successes pertaining to systemic gene therapy with rAAV-9 in dogs (25, 52) could be attributed among other factors to the absence of interactions between this vector and dog G3BP. These interactions could also play a role in vector biodistribution, as was recently shown for liver targeting with adenovirus serotype 5 through binding to coagulation factor X (48). Taking into account that these interactions are truly species specific, this phenomenon should be taken into consideration when studying vector distribution and efficacy in different animal models as well as for toxicology studies.

ACKNOWLEDGMENTS

We thank Olivier Danos, Patrick Dreyfus, and Helge Amthor for helpful discussions and Carole Masurier, Véronique Blouin, Guillaume Précigout, Laëtitia Van Wittenberghe, Béatrice Marolleau, Christophe Georger, Jeremy Rouillon, and the Genethon *in vivo* evaluation core for assistance.

This work was supported by the Association Française contre les Myopathies (AFM), the Duchenne Parent Project France (DPPF), and the Association Monégasque contre les Myopathies (AMM).

REFERENCES

1. **Abernethy TJ, Avery OT.** 1941. The occurrence during acute infections of a protein not normally present in the blood. I. Distribution of the reactive protein in patients' sera and the effect of calcium on the flocculation reaction with C polysaccharide of pneumococcus. J. Exp. Med. **73**:173–182.
2. **Agrawal A, Singh PP, Bottazzi B, Garlanda C, Mantovani A.** 2009. Pattern recognition by pentraxins. Adv. Exp. Med. Biol. **653**:98–116.
3. **Asokan A, et al.** 2010. Reengineering a receptor footprint of adeno-associated virus enables selective and systemic gene transfer to muscle. Nat. Biotechnol. **28**:79–82.
4. **Bish LT, et al.** 2012. Long-term restoration of cardiac dystrophin expression in golden retriever muscular dystrophy following rAAV6-mediated exon skipping. Mol. Ther. **20**:580–589.
5. **Boutin S, et al.** 2010. Prevalence of serum IgG and neutralizing factors against adeno-associated virus (AAV) types 1, 2, 5, 6, 8, and 9 in the healthy population: implications for gene therapy using AAV vectors. Hum. Gene Ther. **21**:704–712.
6. **Boye SE, et al.** 2010. Functional and behavioral restoration of vision by gene therapy in the guanylate cyclase-1 (GC1) knockout mouse. PLoS One **5**:e11306. doi:10.1371/journal.pone.0011306.
7. **Brantly ML, et al.** 2009. Sustained transgene expression despite T lymphocyte responses in a clinical trial of rAAV1-AAT gene therapy. Proc. Natl. Acad. Sci. U. S. A. **106**:16363–16368.
8. **Chenail G, Brown NE, Shea A, Feire AL, Deng G.** 2011. Real-time analysis of antibody interactions with whole enveloped human cytomegalovirus using surface plasmon resonance. Anal. Biochem. **411**:58–63.
9. **Chicheportiche Y, Vassalli P.** 1994. Cloning and expression of a mouse macrophage cDNA coding for a membrane glycoprotein of the scavenger receptor cysteine-rich domain family. J. Biol. Chem. **269**:5512–5517.
10. **Denard J, et al.** 2009. Quantitative proteomic analysis of lentiviral vectors using 2-DE. Proteomics **9**:3666–3676.
11. **Denti MA, et al.** 2006. Body-wide gene therapy of Duchenne muscular dystrophy in the mdx mouse model. Proc. Natl. Acad. Sci. U. S. A. **103**:3758–3763.
12. **DiPrimio N, McPhee SW, Samulski RJ.** 2010. Adeno-associated virus for the treatment of muscle diseases: toward clinical trials. Curr. Opin. Mol. Ther. **12**:553–560.
13. **Drittanti L, Rivet C, Manceau P, Danos O, Vega M.** 2000. High throughput production, screening and analysis of adeno-associated viral vectors. Gene Ther. **7**:924–929.
14. **Friedman J, Trahey M, Weissman I.** 1993. Cloning and characterization of cyclophilin C-associated protein: a candidate natural cellular ligand for cyclophilin C. Proc. Natl. Acad. Sci. U. S. A. **90**:6815–6819.
15. **Garlanda C, Bottazzi B, Bastone A, Mantovani A.** 2005. Pentraxins at the crossroads between innate immunity, inflammation, matrix deposition, and female fertility. Annu. Rev. Immunol. **23**:337–366.
16. **Goyenvalle A, et al.** 2004. Rescue of dystrophic muscle through U7 snRNA-mediated exon skipping. Science **306**:1796–1799.
17. **Gregorevic P, Blankinship MJ, Allen JM, Chamberlain JS.** 2008. Systemic microdystrophin gene delivery improves skeletal muscle structure and function in old dystrophic mdx mice. Mol. Ther. **16**:657–664.
18. **Gregorevic P, et al.** 2004. Systemic delivery of genes to striated muscles using adeno-associated viral vectors. Nat. Med. **10**:828–834.
19. **Groschel B, et al.** 2000. Elevated plasma levels of 90K (Mac-2 BP) immunostimulatory glycoprotein in HIV-1-infected children. J. Clin. Immunol. **20**:117–122.
20. **Hasbrouck NC, High KA.** 2008. AAV-mediated gene transfer for the treatment of hemophilia B: problems and prospects. Gene Ther. **15**:870–875.
21. **Hellstern S, et al.** 2002. Functional studies on recombinant domains of Mac-2-binding protein. J. Biol. Chem. **277**:15690–15696.
22. **Hermens WT, et al.** 1999. Purification of recombinant adeno-associated virus by iodixanol gradient ultracentrifugation allows rapid and reproducible preparation of vector stocks for gene transfer in the nervous system. Hum. Gene Ther. **10**:1885–1891.
23. **Hohenester E, Sasaki T, Timpl R.** 1999. Crystal structure of a scavenger receptor cysteine-rich domain sheds light on an ancient superfamily. Nat. Struct. Biol. **6**:228–232.
24. **Jalkanen K, et al.** 2001. Distinct ligand binding properties of Mac-2-binding protein and mouse cyclophilin [correction of mousephilin] C-associated protein. Eur. J. Immunol. **31**:3075–3084.
25. **Kornegay JN, et al.** 2010. Widespread muscle expression of an AAV9 human mini-dystrophin vector after intravenous injection in neonatal dystrophin-deficient dogs. Mol. Ther. **18**:1501–1508.
26. **Koths K, Taylor E, Halenbeck R, Casipit C, Wang A.** 1993. Cloning and characterization of a human Mac-2-binding protein, a new member of the superfamily defined by the macrophage scavenger receptor cysteine-rich domain. J. Biol. Chem. **268**:14245–14249.
27. **Li H, et al.** 2009. A preclinical animal model to assess the effect of pre-existing immunity on AAV-mediated gene transfer. Mol. Ther. **17**:1215–1224.
28. **Lillicrap D, VandenDriessche T, High K.** 2006. Cellular and genetic therapies for haemophilia. Haemophilia **12**(Suppl. 3):36–41.
29. **Lorain S, et al.** 2008. Transient immunomodulation allows repeated injections of AAV1 and correction of muscular dystrophy in multiple muscles. Mol. Ther. **16**:541–547.
30. **Mingozzi F, High KA.** 2007. Immune responses to AAV in clinical trials. Curr. Gene Ther. **7**:316–324.
31. **Muller SA, et al.** 1999. Domain organization of Mac-2 binding protein and its oligomerization to linear and ring-like structures. J. Mol. Biol. **291**:801–813.
32. **Ng R, et al.** 2010. Structural characterization of the dual glycan binding adeno-associated virus serotype 6. J. Virol. **84**:12945–12957.
33. **Nogues C, et al.** 2010. Characterisation of peptide microarrays for studying antibody-antigen binding using surface plasmon resonance imagery. PLoS One **5**:e12152. doi:10.1371/journal.pone.0012152.
34. **Odom GL, Gregorevic P, Allen JM, Chamberlain JS.** 2010. Gene therapy of mdx mice with large truncated dystrophins generated by recombination using rAAV6. Mol. Ther. **19**:36–45.
35. **Odom GL, Gregorevic P, Allen JM, Finn E, Chamberlain JS.** 2008. Microutrophin delivery through rAAV6 increases lifespan and improves muscle function in dystrophic dystrophin/utrophin-deficient mice. Mol. Ther. **16**:1539–1545.
36. **Pang J, et al.** 2010. Self-complementary AAV-mediated gene therapy restores cone function and prevents cone degeneration in two models of Rpe65 deficiency. Gene Ther. **17**:815–826.
37. **Peiser L, Mukhopadhyay S, Gordon S.** 2002. Scavenger receptors in innate immunity. Curr. Opin. Immunol. **14**:123–128.
38. **Penaud-Budloo M, et al.** 2008. Adeno-associated virus vector genomes persist as episomal chromatin in primate muscle. J. Virol. **82**:7875–7885.
39. **Polyak S, et al.** 2008. Gene delivery to intestinal epithelial cells in vitro and in vivo with recombinant adeno-associated virus types 1, 2 and 5. Dig. Dis. Sci. **53**:1261–1270.
40. **Rapti K, et al.** 2012. Neutralizing antibodies against AAV serotypes 1, 2, 6, and 9 in sera of commonly used animal models. Mol. Ther. **20**:73–83.
41. **Resnick D, Pearson A, Krieger M.** 1994. The SRCR superfamily: a family reminiscent of the Ig superfamily. Trends Biochem. Sci. **19**:5–8.
42. **Sasaki T, Brakebusch C, Engel J, Timpl R.** 1998. Mac-2 binding protein is a cell-adhesive protein of the extracellular matrix which self-assembles into ring-like structures and binds beta1 integrins, collagens and fibronectin. EMBO J. **17**:1606–1613.
43. **Siboo R, Kulisek E.** 1978. A fluorescent immunoassay for the quantification of C-reactive protein. J. Immunol. Methods **23**:59–67.
44. **Smith RH, Levy JR, Kotin RM.** 2009. A simplified baculovirus-AAV expression vector system coupled with one-step affinity purification yields high-titer rAAV stocks from insect cells. Mol. Ther. **17**:1888–1896.
45. **Stone D, et al.** 2008. Biodistribution and safety profile of recombinant adeno-associated virus serotype 6 vectors following intravenous delivery. J. Virol. **82**:7711–7715.
46. **Towne C, Raoul C, Schneider BL, Aebischer P.** 2008. Systemic AAV6 delivery mediating RNA interference against SOD1: neuromuscular transduction does not alter disease progression in fALS mice. Mol. Ther. **16**:1018–1025.
47. **van der Laan LJ, Wang Y, Tilanus HW, Janssen HL, Pan Q.** 2011. AAV-mediated gene therapy for liver diseases: the prime candidate for clinical application? Expert Opin. Biol. Ther. **11**:315–327.

48. **Waddington SN, et al.** 2008. Adenovirus serotype 5 hexon mediates liver gene transfer. Cell **132**:397–409.
49. **Wang M, et al.** 2001. MUSEAP, a novel reporter gene for the study of long-term gene expression in immunocompetent mice. Gene **279**:99–108.
50. **Wright JF.** 2009. Transient transfection methods for clinical adeno-associated viral vector production. Hum. Gene Ther. **20**:698–706.
51. **Wu Z, et al.** 2006. Single amino acid changes can influence titer, heparin binding, and tissue tropism in different adeno-associated virus serotypes. J. Virol. **80**:11393–11397.
52. **Yue Y, et al.** 2008. A single intravenous injection of adeno-associated virus serotype-9 leads to whole body skeletal muscle transduction in dogs. Mol. Ther. **16**:1944–1952.